

This document is downloaded from DR-NTU, Nanyang Technological University Library, Singapore.

Title	Pseudospin dynamics in multimode polaritonic Josephson junctions
Author(s)	Pavlovic, G.; Malpuech, G.; Shelykh, Ivan A.
Citation	Pavlovic, G., Malpuech, G., & Shelykh, I. A. (2013). Pseudospin dynamics in multimode polaritonic Josephson junctions. <i>Physical Review B</i> , 87(12), 125307- .
Date	2013
URL	<a href="http://hdl.handle.net/10220/9913">http://hdl.handle.net/10220/9913</a>
Rights	© 2013 American Physical Society. This paper was published in <i>Physical Review B</i> and is made available as an electronic reprint (preprint) with permission of American Physical Society. The paper can be found at the following official DOI: <a href="http://dx.doi.org/10.1103/PhysRevB.87.125307">http://dx.doi.org/10.1103/PhysRevB.87.125307</a> . One print or electronic copy may be made for personal use only. Systematic or multiple reproduction, distribution to multiple locations via electronic or other means, duplication of any material in this paper for a fee or for commercial purposes, or modification of the content of the paper is prohibited and is subject to penalties under law.

# Pseudospin dynamics in multimode polaritonic Josephson junctions

G. Pavlovic

*International Institute of Physics, Av. Odilon Gomes de Lima, 1722, CEP 59078-400 Capim Macio Natal, RN, Brazil*

G. Malpuech

*Institut Pascal, Photon-N2, Clermont Université and Université Blaise Pascal, CNRS, 63177 Aubière Cedex, France*

I. A. Shelykh

*Physics Department, University of Iceland, Dunhaga-3, IS-107, Reykjavik, Iceland and Division of Physics and Applied Physics, Nanyang Technological University 637371, Singapore*

(Received 30 May 2012; revised manuscript received 12 October 2012; published 11 March 2013)

Using Keldysh-Green function formalism we theoretically analyzed the dynamics of multimode exciton-polariton Josephson junctions. We took into account the spinor nature of polaritons and considered in detail the role of coupling of the fundamental modes with excited states. We demonstrate that the coupling to the reservoir results in a change of the oscillation pattern. In particular, it can lead to renormalization of the oscillation frequency, appearance of higher order harmonics, and induce transition between the regimes of free Josephson oscillations and macroscopic quantum self-trapping.

DOI: [10.1103/PhysRevB.87.125307](https://doi.org/10.1103/PhysRevB.87.125307)

PACS number(s): 71.36.+c, 71.35.Lk, 03.75.Mn

## I. INTRODUCTION

After the theoretical prediction<sup>1</sup> and the experimental detection<sup>2</sup> of Josephson tunneling between two superconductors separated by a thick insulator under the application of an external voltage, analogous quantum oscillations were found between two vessels of superfluid helium connected by a nanoscale aperture.<sup>3</sup> Later on, a similar type of dynamics was described and observed between two weakly coupled cold atoms Bose-Einstein condensates (BECs) created in a double-trap potential.<sup>4,5</sup> Differently from the superconductors and superfluid helium case, the Josephson effect for cold atoms is strongly affected by interparticle interactions.<sup>4</sup> Anharmonic behavior occurs in these systems additionally to common Josephson oscillations. One of the most impressive and special phenomena arising in this system is the macroscopic quantum self-trapping (MQST).<sup>6</sup> If the interaction energy is at least four times larger than the tunneling constant, an initial population imbalance rises the energy in one trap with respect to the other, which suppresses the tunneling current.<sup>6</sup> Bosons do not oscillate anymore from one well to the other, remaining trapped, where they have been initially introduced.

In the so-called Josephson regime, which allows for a mean field classical description of the condensate wave function, the Bosonic Josephson junction (BJJ) is described by the well-known classical Hamiltonian:

$$H = H_0[z(0), \theta(0)] = \Lambda \frac{z(t)^2}{2} - \cos \theta(t) \sqrt{1 - z(t)^2}, \quad (1)$$

written in terms of population imbalance  $z(t) = [N_1(t) - N_2(t)]/[N_1(t) + N_2(t)]$ , where  $N_1$  and  $N_2$  are populations in trap one and trap two, and the phase difference  $\theta(t)$  between BECs. A two-mode approximation including only the lowest energy states of a symmetric double-trap is used in the Hamiltonian (1)<sup>6</sup> which contains a single dimensionless parameter  $\Lambda = U_0 N_T / 2J$ . In the last expression  $J$  figures as Josephson coupling equal to half of the energy splitting between symmetric and antisymmetric states of the

double-trap potential in the linear regime.  $N_T$  is the total population of particles in both traps which interact with characteristic constant  $U_0$ .

Inspecting the phase-space diagram  $(z, \theta)$  of the Hamiltonian (1), one can observe two distinct regions separated by a separatrix line  $H = 1$  (full/red contour in Fig. 1). The value of  $H$  in (1) can be set by choosing the initial conditions  $z(0)$  and  $\theta(0)$ . A delocalized regime will establish if  $H < 1$ . It is characterized by the population imbalance being zero on average [ $\langle z(t) \rangle = 0$ ] and corresponds to cyclic motion on closed orbits (see Fig. 1). Approaching the separatrix from the inner side one starts to deviate from regular circles because of the increasing effect of nonlinearity. Outside the separatrix, where  $H > 1$ , the population imbalance evolves along open lines with small oscillations around a constant mean value  $\langle z(t) \rangle = \text{const}$  indicating the transition to the MQST regime.

In addition to cold atomic gases there are also a few solid state systems in which different quasiparticles when being cooled down at low temperatures form an ordered macroscopically occupied quantum state. One of these systems is the cavity exciton-polariton (polariton) gas. Polariton condensation was observed several years ago in CdTe microcavities at about 20 K.<sup>7,8</sup> The condensation of polaritons also takes place in GaAs,<sup>9,10</sup> GaN,<sup>11,12</sup> and ZnO-based<sup>13</sup> microcavities, in the two latter cases even at room temperature. The possibility of creating BEC under such conditions is extremely interesting from a fundamental point of view. Besides, it opens a way for the design of optoelectronic components, such as polariton lasers<sup>14</sup> and various devices exploiting polariton superfluidity.<sup>15</sup>

Polaritons are two-dimensional quasiparticles that appear due to the strong coupling of excitons in semiconductor quantum well(s) and photons confined within a microcavity structure.<sup>16,17</sup> Peculiar properties of exciton polaritons are consequences of their hybrid, half-light half-matter nature coming from photonic and excitonic constituents respectively. In particular, their ultra-small effective mass, which is typically

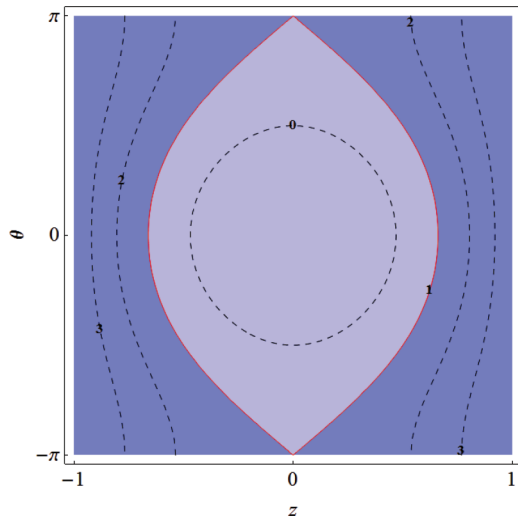


FIG. 1. (Color online) Hamiltonian (1) in the phase space  $(z, \theta)$  for  $\Lambda = 8$ . Contour lines for  $H = 0, 1, 2$ , and  $3$  are labeled. Separatrix is shown with full/red line.

four or five orders of magnitude less than the free electron mass, makes quantum collective phenomena extremely pronounced even at high temperatures (transition to BEC phase is one of the examples). On the other hand polaritons inherit from their excitonic part strong interparticle interactions.

Another prominent feature of polaritons is that the total angular momentum of the polariton state along the structure growth axis (chosen as  $z$  direction)  $J_z^{\text{pol}}$  can take two values ( $J_z^{\text{exc}} = \pm 1$ ).<sup>18</sup> The two values of  $J_z^{\text{pol}} = \pm 1$  (usually referred to as the polariton pseudospin) correspond to mixing of bright excitons ( $J_z^{\text{exc}} = \pm 1$ ) and photons with right or left circular polarizations.

Dark excitons with  $J_z^{\text{exc}} = \pm 2$  are uncoupled from cavity mode due to optical selection rules and thus do not contribute to the formation of a polariton doublet. From the point of view of spin, a polariton is thus a two level system equivalent to an electron or to a photon. Consequently one can apply the pseudospin formalism for the description of the spin dynamics of polaritons. It is convenient to represent the pseudospin state of a polariton system by a point on the Poincaré sphere (also known as Bloch sphere). Importantly, polariton pseudospin unambiguously defines the polarization state of the photoemission from the cavity. The states lying at the poles of the Poincaré sphere correspond to circular polarization of polaritons, the states on the equator to linear polarizations, and all other states to elliptical polarizations.

Being interacting bosons, exciton polaritons can be used to realize a Bosonic Josephson junction. Polaritonic Josephson junctions (PJJs) were considered theoretically in Refs. 19–21 and experimentally in Refs. 22 and 23. Except for Ref. 23, polariton pseudospin was neglected in these works, and only Josephson coupling between the polaritons located in spatially separated traps was included. The introduction of the polarization degree of freedom makes Josephson dynamics far more rich. Indeed, in addition to the coupling between states localized in different traps, two polarization states in a single asymmetric trap can be coupled as well, by a mechanism analogous to TE-TM splitting.<sup>24</sup>

Josephson-type oscillations can occur between different polarizations, a phenomenon which is called intrinsic Josephson effect.<sup>25</sup> Interplay between intrinsic and extrinsic Josephson dynamics can lead to dynamical separation of different polarizations in real space and other intriguing phenomena.<sup>25</sup>

The system of coupled polariton BECs, with their polarization degree of freedom included, is formally similar to binary mixtures of cold atoms condensates in double-trap potentials. There have been several works on the last topic (Refs. 26–30). The principal mechanism of coupling in binary mixtures is due to atomic-atomic scattering of different species, a process which is nonlinear as opposed to pseudospin coupling in polaritonic condensates, which is a linear process resulting in intrinsic Josephson oscillations.

The role of polarization coupling in PJJ was studied for several configurations.<sup>31–33</sup> In most of them, the so-called two-mode approximation was applied, in which only the two lowest levels, one in each of the traps, were considered. In Ref. 33 several modes were included in order to study damping of Josephson oscillations due to the interactions of polaritons with acoustic phonons. However, in this case the separation between two fundamental modes and excited ones was considered to be much greater than characteristic values of blueshifts provided by polariton-polariton interactions, and the transitions to excited modes were only possible due to absorption of phonons.

In this paper we analyze multimode PJJs with confining potential created in such a way that interactions between the lowest and excited levels are not negligible, which is indeed the case in experimental realizations.<sup>23</sup> This kind of coupling has already been considered for Josephson junctions based on atomic BECs.<sup>34</sup> Our goal is to extend the analysis of Ref. 34 for the case of cavity polaritons accounting for the polarization degree of freedom, and clarify the effects of the coupling between the fundamental and excited modes on nonlinear polarization dynamics in PJJs.

## II. MODEL

In Ref. 34, the Keldysh-Green functions technique was employed to study the dynamics of the BJJ with multimode structure. Here we shall follow a similar approach for the description of PJJs with the spin degree of freedom. Because of the spinor nature of polariton condensate in addition to usual Josephson coupling, we have to also consider the coupling between polarization components within different modes of the external potential.

We start by expanding the exciton-polariton field operators  $\hat{\Psi}_{\sigma\pm}(r, t)$  over the complete set of eigenstates  $\{f_1, f_2, \dots\}$  of the double-well potential

$$\hat{\Psi}_{\sigma\pm}(r, t) = f_1(r)\hat{a}_{1\sigma\pm}(t) + f_2(r)\hat{a}_{2\sigma\pm}(t) + \sum_{n=3}^{\infty} f_n(r)\hat{b}_{n\sigma\pm}(t). \quad (2)$$

In the last series  $\hat{a}_{1\sigma\pm}$  and  $\hat{a}_{2\sigma\pm}$  denote the annihilation operators for the lowest modes localized in the traps one and two. The same quantities in the excited level  $n$  are  $\hat{b}_{n\sigma\pm}$  with  $\sigma\pm$  indicating the circular polarization of the state.

The system under study is described by the Hamiltonian being the sum of three terms:

$$\hat{H} = \hat{H}_{\sigma^+} + \hat{H}_{\sigma^-} + \hat{H}_{\sigma^+\sigma^-}. \quad (3)$$

The spin conserving terms  $\hat{H}_{\sigma^+}$  and  $\hat{H}_{\sigma^-}$  are given by the following expressions:

$$\begin{aligned} \hat{H}_{\sigma^\pm} = & \int d^2r \hat{\Psi}_{\sigma^\pm}^\dagger(r,t) \left[ -\frac{\hbar^2}{2m} \Delta + V_{\text{ext}}(r,t) \right] \hat{\Psi}_{\sigma^\pm}(r,t) \\ & + \frac{1}{2} \int d^2r \int d^2r' \hat{\Psi}_{\sigma^\pm}^\dagger(r,t) \hat{\Psi}_{\sigma^\pm}^\dagger(r',t) V(r,r') \\ & \times \hat{\Psi}_{\sigma^\pm}(r',t) \hat{\Psi}_{\sigma^\pm}(r,t), \end{aligned} \quad (4)$$

where  $m$  is the effective mass of the polaritons and  $V_{\text{ext}}(r,t)$  the double-well potential.  $V(r,r') = g\delta(r-r')$  is a contact type interaction described by delta function. The interaction constant can be estimated as  $g \approx E_B a_B^2$ , with  $E_B$  and  $a_B$  being the exciton binding energy and Bohr radius, respectively.<sup>35</sup>

The last term in Eq. (3) accounts for the Josephson-type coupling between particles having opposite pseudospin projections. It can be viewed as the result of the presence of an effective in-plane magnetic field  $\Omega(r)$  arising from the asymmetry of the structure<sup>24</sup> and acting on the polaritons pseudospins. It can be represented as

$$\hat{H}_{\sigma^+\sigma^-} = \int d^2r \hat{\Psi}_{\sigma^+}^\dagger(r,t) \Omega(r) \hat{\Psi}_{\sigma^-}(r,t). \quad (5)$$

After substitution of the expansions (2) into the Hamiltonians (4) and (5) the Hamiltonian (3) can be recast as

$$\hat{H} = \hat{H}^0 + \hat{H}^{\text{exc}} + \hat{H}^{\text{int}}. \quad (6)$$

The first term describes the dynamics of the four fundamental modes (including the polarization degree of freedom), the second term describes the dynamics of the delocalized excited modes, and the last term corresponds to the coupling between the fundamental and excited modes. These terms read:

$$\begin{aligned} \hat{H}^0 = & E_0 \sum_{i;\sigma} \hat{a}_{i\sigma}^\dagger \hat{a}_{i\sigma} + J_0 \sum_{\sigma} (\hat{a}_{1\sigma}^\dagger \hat{a}_{2\sigma} + \hat{a}_{2\sigma}^\dagger \hat{a}_{1\sigma}) \\ & + \frac{U_0}{2} \sum_{i;\sigma} \hat{a}_{i\sigma}^\dagger \hat{a}_{i\sigma}^\dagger \hat{a}_{i\sigma} \hat{a}_{i\sigma} + \Omega_0 \sum_{i;\sigma} \hat{a}_{i\sigma}^\dagger \hat{a}_{i-\sigma}; \end{aligned} \quad (7)$$

$$\begin{aligned} \hat{H}^{\text{exc}} = & \sum_{n,m;\sigma} (E_n + U_{nm} \langle \hat{b}_{m\sigma}^\dagger \hat{b}_{m\sigma} \rangle) \hat{b}_{n\sigma}^\dagger \hat{b}_{n\sigma} \\ & + \sum_{n,m;\sigma} \frac{U_{nm}}{2} (\langle \hat{b}_{m\sigma}^\dagger \hat{b}_{m\sigma} \rangle \hat{b}_{n\sigma} \hat{b}_{n\sigma} + \text{H.c.}) \\ & + \sum_{n;\sigma} \Omega_n \hat{b}_{n\sigma}^\dagger \hat{b}_{n-\sigma}; \end{aligned} \quad (8)$$

$$\begin{aligned} \hat{H}^{\text{int}} = & \sum_{i,n;\sigma} K_n \left[ \frac{1}{2} (\hat{a}_{i\sigma}^\dagger \hat{a}_{i\sigma}^\dagger \hat{b}_{n\sigma} \hat{b}_{n\sigma} + \text{H.c.}) + 2\hat{a}_{i\sigma}^\dagger \hat{a}_{i\sigma} \hat{b}_{n\sigma}^\dagger \hat{b}_{n\sigma} \right] \\ & + \sum_{n;\sigma} 2J_n (\hat{a}_{1\sigma}^\dagger \hat{a}_{2\sigma} + \hat{a}_{2\sigma}^\dagger \hat{a}_{1\sigma}) \hat{b}_{n\sigma}^\dagger \hat{b}_{n\sigma} \\ & + \sum_{n;\sigma} J_n (\hat{a}_{1\sigma}^\dagger \hat{a}_{2\sigma}^\dagger \hat{b}_{n\sigma} \hat{b}_{n\sigma} + \text{H.c.}) \end{aligned} \quad (9)$$

In the above expressions  $E_n$  are the energies of the modes,  $J_0$  is the Josephson coupling strength between the fundamental modes localized in the right and in the left trap of double-well potential,  $\Omega_n$  are the coupling strengths between states of different polarizations at level  $n$ , which leads to the intrinsic Josephson effect,  $U_0$  describes the polariton-polariton interaction in the fundamental modes,  $U_{mn}$  the interactions in excited modes,  $K_n$  the interactions between the fundamental and excited modes, and  $J_n$  describes the renormalization of the Josephson tunneling due to the interaction between the fundamental and excited modes. The parameters entering into the Hamiltonian (6) can be calculated by using the wave functions of localized polariton modes:

$$E_{0(n)} = \int d^2r f_{1,2(n)}^*(r) \left[ -\frac{\hbar^2}{2m} \Delta + V_{\text{ext}}(r) \right] f_{1,2(n)}(r), \quad (10)$$

$$J_0 = \int d^2r f_{1,2}^*(r) \left[ -\frac{\hbar^2}{2m} \Delta + V_{\text{ext}}(r) \right] f_{2,1}(r), \quad (11)$$

$$\begin{aligned} U_0 = & \int d^2r \int d^2r' f_{1,2}^*(r) f_{1,2}^*(r') V(r,r') f_{1,2}(r') f_{1,2}(r) \\ = & g \int d^2r |f_{1(2)}(r)|^4, \end{aligned} \quad (12)$$

$$U_{nm} = g \int d^2r |f_m(r)|^2 |f_n(r)|^2, \quad (13)$$

$$\Omega_{0(n)} = g \int d^2r f_{1\sigma,2\sigma(n\sigma)}^*(r) \Omega(r) f_{1-\sigma,2-\sigma(n-\sigma)}(r), \quad (14)$$

$$K_n = g \int d^2r |f_{1,2}(r) f_n(r)|^2, \quad (15)$$

$$J_n = g \int d^2r f_1^*(r) f_2(r) |f_n(r)|^2. \quad (16)$$

In the part corresponding to the excited states  $\hat{H}^{\text{exc}}$  the interactions can be treated using the mean-field approximation<sup>36</sup>

$$\begin{aligned} \hat{b}_{m\sigma}^\dagger \hat{b}_{n\sigma}^\dagger \hat{b}_{n\sigma} \hat{b}_{m\sigma} = & 2 \langle \hat{b}_{m\sigma}^\dagger \hat{b}_{m\sigma} \rangle \hat{b}_{n\sigma}^\dagger \hat{b}_{n\sigma} + \langle \hat{b}_{m\sigma}^\dagger \hat{b}_{m\sigma} \rangle \langle \hat{b}_{n\sigma}^\dagger \hat{b}_{n\sigma} \rangle \\ & + \langle \hat{b}_{m\sigma} \hat{b}_{m\sigma} \rangle \hat{b}_{n\sigma}^\dagger \hat{b}_{n\sigma}^\dagger. \end{aligned} \quad (17)$$

In the model under study here, coupling characterized by constant  $J_0$  is present only between spatially localized modes, whereas the excited states are spatially delocalized and thus cannot have extrinsic Josephson oscillations. The intrinsic Josephson oscillations have not such exclusivity and appear in all modes of the system.

In order to obtain a closed system of dynamical equations describing interacting multimode PJJ, we write its Keldysh-Green propagators in the following representation

$$\tilde{G}_{\alpha\beta}(t,t') = \begin{pmatrix} \hat{G}_{\alpha\beta\sigma\sigma}(t,t') & \hat{G}_{\alpha\beta\sigma-\sigma}(t,t') \\ \hat{G}_{\alpha\beta-\sigma\sigma}(t,t') & \hat{G}_{\alpha\beta-\sigma-\sigma}(t,t') \end{pmatrix}, \quad (18)$$

where general indices  $\alpha$  and  $\beta$  become  $i$  or  $j$  for the ground states taking values 1 or 2 as there are two traps. The excited states are counted by associating  $m$  or  $n$  with  $\alpha$  or  $\beta$ . As previously indices  $\pm\sigma$  denote pseudospin degrees of freedom. The elements of the above matrix (18) are themselves  $2 \times 2$  block matrices of the form

$$i\hat{G}_{\alpha\beta\sigma\sigma}(t,t') = \begin{bmatrix} G_{\alpha\beta\sigma\sigma}(t,t') & F_{\alpha\beta\sigma\sigma}(t,t') \\ \bar{F}_{\alpha\beta\sigma\sigma}(t,t') & \bar{G}_{\alpha\beta\sigma\sigma}(t,t') \end{bmatrix}, \quad (19)$$

with its own elements being

$$G_{nm\sigma\sigma}(t, t') = \langle \mathcal{T} \hat{b}_{n\sigma}(t) \hat{b}_{m\sigma}^\dagger(t') \rangle \quad (20)$$

$$F_{nm\sigma\sigma}(t, t') = \langle \mathcal{T} \hat{b}_{n\sigma}(t) \hat{b}_{m\sigma}(t') \rangle, \quad (21)$$

in these two cases and similarly for the remaining correlators.

Time-ordering  $\mathcal{T}$  in the previous formulas is performed on the Keldysh contour.<sup>37</sup> It appears because of nonadiabatic switching of the Josephson coupling at initial time. With such a kind of irreversibility it is not possible to guarantee that the system will stay in equilibrium for asymptotically large times.<sup>38</sup> Hence, the time contour in the Keldysh formalism is adapted in that way that the system evolves forwardly to some finite point on the time axis and then returns backwardly to the initial state. The Keldysh time ordered product of two operators, for example, of the operators  $\hat{b}_n$  and  $\hat{b}_m$ , reads

$$\langle \mathcal{T} [\hat{b}_m(t) \hat{b}_n(t')] \rangle = \theta(t, t') \langle \hat{b}_m(t) \hat{b}_n(t') \rangle + \theta(t', t) \langle \hat{b}_n(t') \hat{b}_m(t) \rangle, \quad (22)$$

where  $\theta(t, t')$  is the Heaviside step function defined on the Keldysh contour for two arbitrary times  $t$  and  $t'$  in a way that it is always unity when the first argument is later than the second one, and zero otherwise. In this sense the first Green function in the formula (22) is called “greater,” denoted with  $F^>(t, t')$  and the second one is “lesser” Green function  $F^<(t, t')$ . They act only on the forward or the backward Keldysh contour branch.

Using Wigner transformation matrix elements  $G_{\alpha\beta\sigma\sigma}(t, t')$  can be written in terms of center of “mass” and “relative” time coordinates  $T = (t + t')/2$  and  $\tau = t - t'$ . We are interested here in the external and internal Josephson dynamics which are slower processes than the other ones occurring in the system so that we can work in the limit  $\tau = 0$ . Thus, the new matrix elements  $G_{\alpha\beta\sigma\sigma}(T, \tau)$  only depend on the macroscopical time  $T$ .<sup>34</sup> According to the expression (22) we will deal only with “lesser” functions  $F^<(T)$  and  $G^<(T)$ .

Equations of motion techniques combined with the use of the mean-field approximation allow us to obtain one closed system of equations for the Keldysh-Green functions defined by Eq. (19):

$$i \frac{dG_{n\sigma n\sigma}^<} {dT} = \Xi_{n\sigma} \bar{F}_{n\sigma n\sigma}^< - \bar{\Xi}_{n\sigma} F_{n\sigma n\sigma}^< - \Omega_n (G_{n\sigma n-\sigma}^< - G_{n-\sigma n\sigma}^<), \quad (23)$$

$$\left( i \frac{d}{dT} + \Upsilon_{n\sigma} - \Upsilon_{n-\sigma} \right) G_{n\sigma n-\sigma}^< = 2\Xi_{n\sigma} \bar{F}_{n\sigma n-\sigma}^< - 2\bar{\Xi}_{n\sigma} F_{n\sigma n-\sigma}^< - \Omega_n (G_{n\sigma j\sigma}^< - G_{n-\sigma n-\sigma}^<), \quad (24)$$

$$\left( i \frac{d}{dT} - 2E_{n\sigma} - 2\Upsilon_{n\sigma} \right) F_{n\sigma n\sigma}^< = 2\bar{\Xi}_{n\sigma} G_{n\sigma n\sigma}^< + 2\Xi_{n\sigma} \bar{G}_{n\sigma n\sigma}^< - \Omega_n F_{n\sigma n-\sigma}^<, \quad (25)$$

$$\left( i \frac{d}{dT} + 2E_{n\sigma} + \Upsilon_{n\sigma} + \Upsilon_{n-\sigma} \right) F_{n\sigma n-\sigma}^< = -2(\Xi_{n\sigma} - \bar{\Xi}_{n-\sigma}) G_{n\sigma n-\sigma}^< - \Omega_n (F_{n\sigma n\sigma}^< + F_{n-\sigma n-\sigma}^<), \quad (26)$$

where  $n = 3, 4, \dots$  stands for the  $n$ th excited level. Dynamics of the fundamental states are given by the following expressions:

$$i \frac{dA_{j-\sigma i\sigma}^<} {dT} = \left( E_0 + U_0 G_{i\sigma i\sigma}^< + 2 \sum_{n\sigma} K_n G_{n\sigma n\sigma}^< \right) A_{j-\sigma i\sigma}^< + \left( J_0 + 2 \sum_{n\sigma} J_n G_{n\sigma n\sigma}^< \right) A_{j-\sigma j\sigma}^< + i \sum_{n\sigma} (K_n \bar{B}_{j-\sigma i\sigma}^< + J_n \bar{B}_{j-\sigma j\sigma}^<) F_{n\sigma n\sigma}^< - \Omega_0 A_{j-\sigma i-\sigma}^<, \quad (27)$$

with  $i, j = 1, 2$ , and  $A, B = G$  or  $F$  ( $A \neq B$ ). The self-energies  $\Upsilon$  and  $\Xi$  are

$$-i\Upsilon_{n\sigma} = U^* \sum_m G_{m\sigma m\sigma}^< + 2K_n (G_{1\sigma 1\sigma}^< + G_{2\sigma 2\sigma}^<) + 2J_n (G_{1\sigma 2\sigma}^< + G_{2\sigma 1\sigma}^<), \quad (28)$$

$$-i\Xi_{n\sigma} = \frac{U^*}{2} \sum_m F_{m\sigma m\sigma}^< + \frac{K_n}{2} (F_{1\sigma 1\sigma}^< + F_{2\sigma 2\sigma}^<) + J_n F_{1\sigma 2\sigma}^<. \quad (29)$$

The normal and anomalous self-energies, equations (28) and (29), represent the energy renormalizations entering in the diagonal and off-diagonal propagators in the matrix (19) due to particle-particle interactions. For simplicity we take them diagonal in the excited level index  $n$  neglecting collisions between particles situated at different reservoir levels,  $U_{nm} = U^* \delta_{nm}$ .

The system of equations (23)–(29) is a closed system of nonlinear first order ordinary differential equations which can be solved numerically. The corresponding analysis is presented in the next section.

### III. RESULTS AND DISCUSSIONS

We consider a PJJ with parameters similar to those used in Ref. 25. To estimate polariton-polariton interactions in the localized modes  $U_0$  we consider a Ga-As based structure taking the exciton Bohr radius  $a_B = 35 \text{ \AA}$ , the exciton binding energy  $E_B = 25 \text{ meV}$ , and considering the trap with a lateral size of  $50 \text{ \mu m}$ . The system of equations (23)–(29) was analyzed numerically. All Keldysh Green functions for the reservoir are initially set to zero, with the exception of those representing occupancies in the levels.

Their values at  $T = 0$  can be easily found with the help of the expression (30) knowing the polariton densities and the fraction of particles out of the condensate, given in the legends

below. The population of the reservoir modes higher than the first excited one could be safely unvalued at  $T = 0$  from the following reasoning. In our model we do not consider density-density interactions between higher levels (Ref. 34):  $U_{nm} \rightarrow 0$  when  $m \neq n$ . Thus, dynamics on the  $n_{th}$  level is autonomous from the one occurring in the level  $m$ . Furthermore, the overlap integral between  $n_{th}$  and  $i_{th}$  modes naturally decreases with  $n$  and by formulas (15) and (16) yields quite small values for  $K_n$  and  $J_n$  for the modes higher than the first reservoir one. Inclusion of the last constants and initial populations in the higher level would eventually give very small quantitative modification of the ground state oscillations and as such are side effects not of principal interest.

In cold atoms condensates it was discovered (Ref. 34) that the interactions with reservoir lead to chaotization of the Josephson oscillations after initially regular dynamics. The effect is due to the intensive exchange of particles between the fundamental states and multimode reservoir with the excited states. Here we consider time intervals smaller than those necessary for the transition to the chaotic regime. The reason is that polaritons have finite lifetimes, and in the regime of pulsed excitation they will simply disappear before the system will demonstrate the characteristics of chaos.<sup>25</sup>

The quantity

$$\rho_{i(n)}(T) = \frac{1}{N_T} [G_{i(n)\sigma+i(n)\sigma^+}^<(T) - G_{i(n)\sigma-i(n)\sigma^-}^<(T)] \quad (30)$$

describes the circular polarization degree of the state  $i(n)$  where  $N_T = \sum_{i,n,\sigma} G_{i\sigma i\sigma} + G_{n\sigma n\sigma}$  is the total number of particles. We consider an external double trap potential created in such a way that there is a 200  $\mu\text{eV}$  gap between its modes.

For a while, we neglect the extrinsic Josephson coupling putting  $J_0 = 0$  and also  $J_n = 0$  (Fig. 2). Panels (a) and (b)

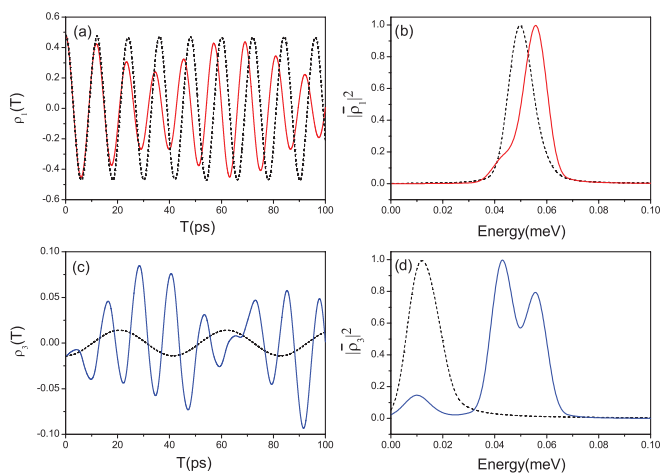


FIG. 2. (Color online) Panels (a) and (b): profile of the intrinsic Josephson oscillations of circular polarization degree at the fundamental states and its Fourier power spectrum for  $\Omega_0 = 100 \mu\text{eV}$ . Panels (c) and (d): profile of the intrinsic Josephson oscillations of circular polarization degree at the first excited state and its Fourier power spectrum. Dashed lines correspond to the absence of the coupling between the fundamental modes and excited states,  $K_n = 0$ . Solid lines correspond to the case  $K_n = 0.3U_0$ . Total polariton density is  $n_{\text{tot}} = 1.87 \times 10^{11} \text{ cm}^{-2}$  and the fraction in the reservoir is  $n_r = 0.10n_{\text{tot}}$ .

show a profile of the oscillations of the circular polarization degree in the fundamental states corresponding to the intrinsic Josephson effect and the corresponding Fourier power spectrum. The dashed line corresponds to the case when the coupling with the excited states is switched off, while the solid line accounts for this coupling. One can see that the introduction of the term  $K_n$  renormalizes the frequency of the oscillations within the ground level. The effect remains quite weak, as the population fraction in the excited levels is rather small, about ten percent for the first excited level. However, an additional beating in the oscillations is present, visible in Fig. 2(b) as a shoulder in the Fourier spectrum. The coupling effect becomes more pronounced if one monitors the intrinsic Josephson dynamics of circular polarization at the first excited state, shown in panels (c) and (d). The interaction with the fundamental modes changes the oscillation pattern of the excited modes radically. The effect is clearly seen on the panel (d) showing Fourier power spectrum of the oscillations. Account of the terms  $K_n$  leads to the appearance of higher harmonics in the spectrum. Besides, instead of the intrinsic Josephson oscillations with zero time average, as happens when reservoir effects are not treated, here a regime establishes in which  $\langle \rho_{i(n)}(T) \rangle \neq 0$ . Note that in the absence of coupling  $K_n$  the frequencies of the intrinsic oscillations in the ground state and the reservoir are different [dashed lines in panels (a) and (c)], although the polarization couplings are equal:  $\Omega_0 = \Omega_n$ . It is the result of the renormalization of the oscillation frequency for the fundamental mode due to nonlinearities, which are negligible in the reservoir where the number of polaritons is considerably lower. Taking into account the reservoir-fundamental mode coupling makes the frequencies of intrinsic Josephson oscillations comparable for all modes of the system.

Figure 3 illustrates the behavior of the polarization degree in the MQST regime for the intrinsic Josephson effect, including interaction with the reservoir. Contrary to the situation analyzed in Fig. 2, particle-particle interactions dominate over Josephson coupling of the fundamental mode. The profiles of the oscillations of the circular polarization degree for the fundamental modes are shown in the top part of panel (a). The solid line corresponds to the case  $K_n \neq 0$  and the dashed one for  $K_n = 0$ . The dashed line shows oscillations with a single frequency, usual for the MQST regime in the two-mode PJJ. The introduction of the coupling with the excited level leads to the appearance of the two additional peaks in the Fourier spectrum, as is shown on panel (b). As in the regime of linear Josephson oscillations there is a beating in the time average of the circular polarization degree. It starts to oscillate instead of keeping a constant value  $\langle \rho_1(T) \rangle \neq \text{const}$ . Similar trends can be seen for the dynamics of the excited level, illustrated by the lower curves in panel (a) and the thick (blue) line in panel (b). In Ref. 25 it was found that the transition from MQST to a regime of free Josephson oscillations occurs when the finite lifetime of polaritons is taken into account. In present analysis long lifetimes and strong nonlinearities in the ground state well protect polaritons from fast decay and this transition.

Finally, we consider the scenario in which two fundamental modes localized in traps one and two, initially elliptically polarized, are coupled with each other by means of extrinsic Josephson tunneling  $J$ . It was already pointed out that spatial

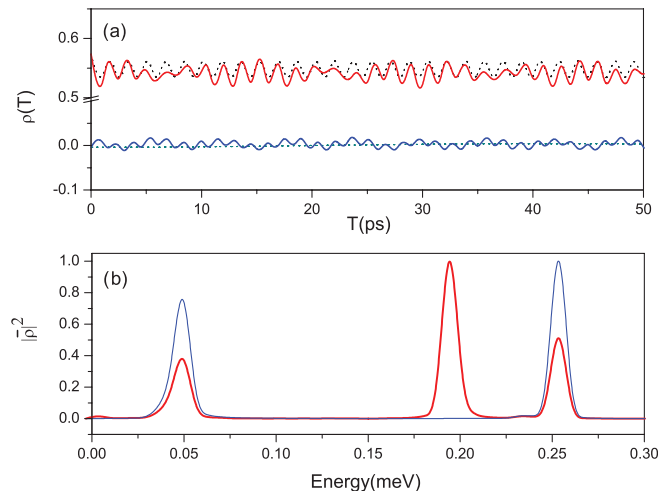


FIG. 3. (Color online) Top of panel (a) shows the polarization degree of the intrinsic Josephson oscillations in the fundamental mode for  $\Omega_0 = 20 \mu\text{eV}$ . Bottom of panel (a) shows the same quantity in the reservoir. Dashed lines:  $K_n = 0$ . Thick/blue and solid/red lines are calculated for  $K_3 = 0.3U_0$ . Panel (b) shows corresponding Fourier power spectrum when the interactions are present (red/solid for the fundamental mode, blue/thick for the reservoir). Total polariton density is  $n_{\text{tot}} = 1.45 \times 10^{12} \text{ cm}^{-2}$  with the reservoir fraction  $n_r = 0.19n_{\text{tot}}$ .

separation of polarization occurs in this case<sup>25</sup> for sufficiently high polariton densities and circular polarization degrees. In this regime the dominant polarization component is trapped in one of the wells (dotted line in lower panel of Fig. 4), while the other one undergoes Josephson oscillations (dotted line in the upper part of Fig. 4). The coupling to the excited states induces an extra pseudospin-conserving exchange of particles from one well to another, assisted by the coupling term  $J_n$  in Eq. (9). The influence of this term is illustrated in Fig. 4 by solid red and blue lines corresponding to  $J_n = 0.1U_0$  and  $J_n = 0.3U_0$ . The presence of the reservoir-assisted term results in the trapping of the minor component which would otherwise freely oscillate. This transition is provided by the competition between two effects: the classical Josephson tunneling  $J$  and the reservoir-assisted coupling given by  $J_n$ . The major polarization component remains relatively robust with respect to the influence of the reservoir-assisted coupling. Note that in the hypothetical case of positive  $J$  the result will be opposite to the one considered here: The reservoir-assisted terms will increase the absolute value of the effective tunneling constant,

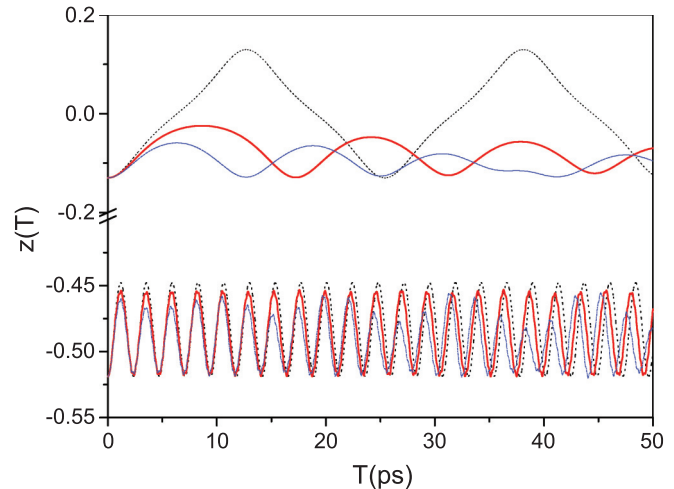


FIG. 4. (Color online) Upper part: Josephson oscillations of the population imbalances between two traps for the minor polarization component. Lower part: Josephson oscillations of the population imbalances between two traps for the major polarization component.  $J_0 = 50 \mu\text{eV}$ . Dashed line: no reservoir-assisted coupling,  $J_n = 0$ . Red line:  $J_3 = 0.1U_0$ , blue line  $J_3 = 0.2U_0$ . Total polariton density in the minor polarization component is  $n_{\text{tot}}^{-\sigma} = 2.43 \times 10^{11} \text{ cm}^{-2}$  with the reservoir fraction  $n_r^{-\sigma} = 0.04n_{\text{tot}}^{-\sigma}$  and  $n_{\text{tot}}^{\sigma} = 9.41 \times 10^{11} \text{ cm}^{-2}$  with  $n_r^{\sigma} = 0.01n_{\text{tot}}^{\sigma}$  for the major polarization component.

thus contributing to the destruction of the MQST regime for the main polarization component.

#### IV. CONCLUSIONS

In conclusion, we analyzed polarization dynamics in multi-mode polaritonic Josephson junctions. We have found that the coupling between fundamental and excited modes changes the patterns of intrinsic and extrinsic Josephson oscillations, leading to the appearance of higher harmonics and transitions between Josephson and MQST regimes.

#### ACKNOWLEDGMENTS

The authors thank D.D. Solnyshkov and N. Gippius for stimulating discussions and I. Gordeliy and A. Sharma for reading of the manuscript. The work was supported by FP7 IRSES projects “SPINMET” and “POLAPHEN” and Rannis “Center of excellence in polaritonics.” G.P. is supported by Science Without Borders Linha 2.2-BJT(402324/2012-9) project.

<sup>1</sup>B. D. Josephson, *Phys. Lett.* **1**, 251 (1962).

<sup>2</sup>A. G. Likharev, *Rev. Mod. Phys.* **51**, 101 (1979).

<sup>3</sup>S. V. Pereverzev, A. Loshak, S. Backhaus, J. C. Davis, and R. E. Packard, *Nature (London)* **388**, 449 (1997).

<sup>4</sup>M. Albiez, R. Gati, J. Fölling, S. Hunsmann, M. Cristiani, and M. K. Oberthaler, *Phys. Rev. Lett.* **95**, 010402 (2005).

<sup>5</sup>S. Levy, E. Lahoud, I. Shomroni, and J. Steinhauer, *Nature (London)* **449**, 579 (2007).

<sup>6</sup>A. Smerzi, S. Fantoni, S. Giovanazzi, and S. R. Shenoy, *Phys. Rev. Lett.* **79**, 4950 (1997); G. J. Milburn, J. Corney, E. M. Wright, and

D. F. Walls, *Phys. Rev. A* **55**, 4318 (1997); S. Raghavan, A. Smerzi, S. Fantoni, and S. R. Shenoy, *ibid.* **59**, 620 (1999).

<sup>7</sup>J. Kasprzak, M. Richard, S. Kundermann, A. Baas, P. Jeambrun, J. M. J. Keeling, F. M. Marchetti, M. H. Szymaska, R. André, J. L. Staehli, V. Savona, P. B. Littlewood, B. Deveaud, and L. S. Dang, *Nature (London)* **443**, 409 (2006); J. Kasprzak, R. André, L. S. Dang, I. A. Shelykh, A. V. Kavokin, Y. G. Rubo, K. V. Kavokin, and G. Malpuech, *Phys. Rev. B* **75**, 045326 (2007).

<sup>8</sup>R. Huang, Y. Yamamoto, R. André, J. Bleuse, M. Muller, and H. Ulmer-Tuffigo, *Phys. Rev. B* **65**, 165314 (2002).

- <sup>9</sup>R. Balili, V. Hartwell, D. Snoke, L. Pfeiffer, and K. West, *Science* **316**, 1007 (2007).
- <sup>10</sup>E. Wertz, L. Ferrier, D. D. Solnyshkov, P. Senellart, D. Bajoni, A. Miard, A. Lemaître, G. Malpuech, and J. Bloch, *Appl. Phys. Lett.* **95**, 051108 (2009).
- <sup>11</sup>J. Levrat, R. Butté, E. Feltin, J.-F. Carlin, N. Grandjean, D. Solnyshkov, and G. Malpuech, *Phys. Rev. B* **81**, 125305 (2010).
- <sup>12</sup>J. J. Baumberg, A. V. Kavokin, S. Christopoulos, A. J. D. Grundy, R. Butté, G. Christmann, D. D. Solnyshkov, G. Malpuech, G. Baldassarri Höger von Högersthal, E. Feltin, J.-F. Carlin, and N. Grandjean, *Phys. Rev. Lett.* **101**, 136409 (2008).
- <sup>13</sup>F. Li, L. Orosz, O. Kamoun, S. Bouchoule, C. Brimont, P. Disseix, T. Guillet, X. Lafosse, M. Leroux, J. Leymarie, M. Mexis, M. Mihailovic, F. Réveret, D. Solnyshkov, J. Zuniga-Perez, and G. Malpuech, [arXiv:1207.7172](https://arxiv.org/abs/1207.7172).
- <sup>14</sup>A. Imamoglu and J. R. Ram, *Phys. Lett. A* **214**, 193 (1996).
- <sup>15</sup>T. C. H. Liew, I. A. Shelykh, and G. Malpuech, *Physica E* **43**, 1543 (2011).
- <sup>16</sup>J. J. Hopfield, *Phys. Rev.* **112**, 1555 (1958).
- <sup>17</sup>C. Weisbuch, M. Nishioka, A. Ishikawa, and Y. Arakawa, *Phys. Rev. Lett.* **69**, 3314 (1992).
- <sup>18</sup>I. A. Shelykh, A. V. Kavokin, Y. G. Rubo, T. C. H. Liew, and G. Malpuech, *Semicond. Sci. Technol.* **25**, 013001 (2010).
- <sup>19</sup>M. Wouters and I. Carusotto, *Phys. Rev. Lett.* **99**, 140402 (2007).
- <sup>20</sup>M. Wouters, *Phys. Rev. B* **77**, 121302 (2008).
- <sup>21</sup>D. Sarchi, I. Carusotto, M. Wouters, and V. Savona, *Phys. Rev. B* **77**, 125324 (2008).
- <sup>22</sup>K. G. Lagoudakis, B. Pietka, M. Wouters, R. André, and B. Deveaud-Plédran, *Phys. Rev. Lett.* **105**, 120403 (2010).
- <sup>23</sup>M. Galbiati, L. Ferrier, D.D. Solnyshkov, D. Tanese, E. Wertz, A. Amo, M. Abbarchi, P. Senellart, I. Sagnes, A. Lemaître, E. Galopin, G. Malpuech, and J. Bloch, *Phys. Rev. Lett.* **108**, 126403 (2012).
- <sup>24</sup>I. L. Aleiner and E. L. Ivchenko, *JETP Lett.* **55**, 692 (1992).
- <sup>25</sup>I. A. Shelykh, D. D. Solnyshkov, G. Pavlovic, and G. Malpuech, *Phys. Rev. B* **78**, 041302(R) (2008).
- <sup>26</sup>G. Mazzarella, M. Moratti, L. Salasnich, M. Salerno, and F. Toigo, *J. Phys. B* **42**, 125301 (2009).
- <sup>27</sup>I. I. Satija, R. Balakrishnan, P. Naudus, J. Heward, M. Edwards, and C. W. Clark, *Phys. Rev. A* **79**, 033616 (2009).
- <sup>28</sup>B. Juliá-Díaz, M. Guilleumas, M. Lewenstein, A. Polls, and A. Sanpera, *Phys. Rev. A* **80**, 023616 (2009).
- <sup>29</sup>R. Citro, A. Naddeo, and E. Orignac, *J. Phys. B* **44**, 115306 (2011).
- <sup>30</sup>S. N. Burmistrov, *Phys. Rev. A* **83**, 063627 (2011).
- <sup>31</sup>D. D. Solnyshkov, R. Johné, I. A. Shelykh, and G. Malpuech, *Phys. Rev. B* **80**, 235303 (2009).
- <sup>32</sup>D. Read, Y. G. Rubo, and A. V. Kavokin, *Phys. Rev. B* **81**, 235315 (2010).
- <sup>33</sup>E. B. Magnusson, H. Flayac, G. Malpuech, and I. A. Shelykh, *Phys. Rev. B* **82**, 195312 (2010).
- <sup>34</sup>M. T. Martínez, A. Posazhennikova, and J. Kroha, *Phys. Rev. Lett.* **103**, 105302 (2009).
- <sup>35</sup>C. Ciuti, V. Savona, C. Piermarocchi, A. Quattropani, and P. Schwendimann, *Phys. Rev. B* **58**, 7926 (1998).
- <sup>36</sup>A. Griffin, *Phys. Rev. B* **53**, 9341 (1996).
- <sup>37</sup>J. Rammer and H. Smith, *Rev. Mod. Phys.* **58**, 323 (1986).
- <sup>38</sup>H. Haug and A. P. Jauho, *Quantum kinetics in transport and optics of semiconductors* (Springer, Berlin, 1996).